3rd URSI AT-AP-RASC, Gran Canaria, 29 May – 3 June 2022

Statistical properties of mid-latitude TEC time series observed during rapidly developing short-term geomagnetic storms: A contribution to GNSS-related TEC predictive model development

Nenad Sikirica*[(1,2)], Weinmin Zhen[(3)], and Renato Filjar[(2,4)]
(1) PhD student, Faculty of Maritime Studies, University of Rijeka, Rijeka, Croatia
(2) Krapina University of Applied Sciences, Krapina, Croatia
(3) China Research Institute of Radiowave Propagation, Qingdao, China
(4) Faculty of Engineering, University of Rijeka, Rijeka, Croatia

Abstract

Total Electron Content (TEC) affects GNSS positioning accuracy due to its effects on GNSS pseudorange measurement. GNSS resilience against the ionospheric effects requires improved accuracy of TEC predictive model. Here a contribution to the subject of self-adaptive positioning environment-aware TEC predictive model development is provided trough statistical analysis of mid-latitude TEC time series observed during rapidly developing short-term geomagnetic storms. Statistical properties of TEC sets and time series are examined to address similarities in range, variability, and information content in order to establish rapidly developing short-term geomagnetic storms as a separate class of the ionospheric event cases, with potential to degrade GNSS positioning accuracy. Results of the analysis show cases of rapidly developing short-term geomagnetic storm share similar statistical properties, notably Shannon entropy and spike index, of TEC observations, which renders them eligible to be addressed with a common TEC prediction model to rise GNSS resilience against the ionospheric effects.

1. Introduction

Total Electron Content (TEC) is a product of ionospheric conditions with direct effects on the operation and performance of numerous technology systems, including Global Navigation Satellite System (GNSS) [1, 4]. GNSS is recognised as a component of national infrastructure, and an enabler of a raising number of technology and socio-economic applications (systems and services) [4]. The ionospheric effects on GNSS positioning performance remain an inherent vulnerability of GNSS, which requires mitigation to ensure the GNSS positioning performance [1, 6]. A range of the GNSS ionospheric effects mitigation method has been developed to alert and compensate for both bias and random effects of ionospheric disturbances on GNSS position estimation accuracy, including TEC disturbance detection methods [2], standard GNSS ionospheric delay correction models [3], and GNSS augmentation systems and services [1, 4]. GNSS correction models are of the global nature, and consider ionospheric conditions in an averaged spatio-temporal manner, thus failing to address local disturbances, especially those of a short duration [4, 6]. GNSS augmentation systems and services require substantial investments and efforts in establishment and operations [4]. A positioning environment-aware self-adapting GNSS position estimation process has been recently proposed, based on positioning environment situation awareness and utilisation of statistical learning-based ionospheric correction models, to overcome the shortcomings in traditional GNSS position estimation process [1, 3, 4]. Development of self-adaptation to different ionospheric conditions requires characterisation of classes of ionospheric events [1]. Here we contribute to the subject by determination and analysis of statistical properties of the mid-latitude TEC observed during rapidly developing short-term geomagnetic storms, as the class of ionospheric events the GNSS positioning performance is substantially vulnerable from, due to spatio-temporal averaged nature of the existing GNSS ionospheric correction models.

This manuscript reads as follows. This Section introduces the problem and the research motivation. Section 2 outlines the scope and methodology used in research, including comprehensive descriptions of statistical methods used. Section 3 details the material, including raw GNSS observation data source, TEC determination, and case scenarios. Section 4 presents the research results. Section 5 inferes and discusses findings and contributions, while placing them into structure of the self-adaptive GNSS ionospheric effects mitigation mehod using a GNSS positioning environment-aware position estimation process.

2. Method

TEC is directly related to the GNSS ionospheric delay, an error in GNSS pseudorange measurement [1, 3, 4]. The GNSS pseudorange measurement error propagates into the GNSS positioning error in the GNSS position estimation process [3, 4, 6]. It may be shown that a direct proportionality exists between the observed GNSS pseudorange measurement error and the TEC encountered by a satellite signal on its propagation path between a satellite and a receiver aerials. TEC results from the ionospheric conditions, rather than being a descriptor of them [6].

Several methods are known for TEC estimation. Using a reverse engineering approach, TEC may be determined using a simultaneous dual-frequency GNSS pseudorange measurement approach, defined for authorised GNSS users, and not available to mass market single-frequency GNSS receivers [6]. Dual-frequency GNSS TEC estimation model utilises simultaneously observed GNSS pseudoranges, $\rho(f_1)$ and $\rho(f_2)$, at two frequencies of radio wave carriers, f_1 and f_2, with the satellite and receiver biases, b_s and b_r, respectively, accounted for, as denoted in (1) [6].

$$TEC = \frac{k_h \cdot k_f}{40.31} \cdot \left[\rho(f_2) - \rho(f_1) - b_s - b_r \right] \quad (1)$$

The GNSS satellite biases are regularly determined by the international academic institutions, such as University of Bern's Center for Orbit Determination in Europe (https://www.aiub.unibe.ch/research/code___analysis_center/index_eng.html), as a service to scientific community. The GNSS receiver biases are generally estimated using bespoke algorithms related to a particular dual-frequency receiver [6].

The height parameter k_h in (1) is determined for every GNSS satellite pseudorange based on the elevation angle, E, as seen from the receiver's position perspective, and the receiver's height above the mean sea level h, as expressed with (2) [6].

$$k_h = \sqrt{1 - \left(\frac{R_{Earth}}{R_{Earth} + h} \cdot \cos(E) \right)^2} \quad (2)$$

The frequency parameter k_f is determined by carrier frequencies f_1 and f_2 used for TEC estimation, as expressed with (3) [6].

$$k_f = \frac{f_1^2 \cdot f_2^2}{f_1^2 - f_2^2} \quad (3)$$

We utilise the GPS-TEC software ver. 3.0 for TEC estimation from the raw GPS pseudorange observations, developed by Dr Gopi Seemala (https://seemala.blogspot.com/). The GPS-TEC software compensates the receiver bias using the internal algorithm, based on the averaged night-time TEC values. The algorithm estimates TEC as the vertical TEC average of vertical TEC estimates from all visible satellites.

Statistical analysis of TEC observations derived using the procedure (1), (2), (3) conducted in this research include the exploratory statistical analysis [5] of the TEC sets, and determination and interpretation of TEC time series statistical properties: (Shannon) entropy [5] and spike index [5].

Exploratory statistical analysis results in a separate determination of median and quartiles of the related TEC set, summarised in box-and-whisker plots [5].

Shannon, or information, entropy is assessed as a measure of randomness in the signal, with values close to zero pointing to good predictability of the process that creates the signal under observations. The original Shannon expression is modified as to suit estimation of the information entropy of a signal, as expressed in (4) [5].

$$e = - \int_{-\pi}^{\pi} \hat{f}(\lambda) \cdot \log \hat{f}(\lambda) \, d\lambda \quad (4)$$

Determination of the *spike index* requires derivation of the random component of a time series, here performed by time-series decomposition using Loess (stl) method [5]. The spike index is determined as variance of the leave-one-out validation variances of the random component of decomposition of the time series under observation. Spike index refers to requirements for smoothness in the model of the observed time series [5].

This research utilises a bespoke statistical analysis software we developed in the open-source R environment for statistical computing (https://www.r-project.org/), based on (4) and spike index determinationmethods implemented in the R library *tsfeatures* developed by Professor Rob J Hyndman et al (https://pkg.robjhyndman.com/tsfeatures/index.html, https://cran.r-project.org/package=tsfeatures).

3. Material

This research utilise raw dual-frequency GPS pseudorange observations collected at the International GNSS Service (IGS) (https://igs.org/) in selected cases of rapidly developing short-term geomagnetic storms.

The IGS network of reference GNSS stations serves scientists with the provision of raw GNSS observations (code and phase) collected with 30 s sampling rate throught a day, every day in the year. The IGS reference station set-up is designed to minimise all the other adverse effects on GNSS observations, such as tropospheric delay and mutipath effects, while leaving the real ionospheric effects intact within the GNSS observations. We selected the Ohrid, North Macedonia reference station as the source of observations used in this research. Figure 1 depicts the position of the Ohrid, North Macedonia reference station in mid-latitude region.

Selection of the cases of rapidly developing short-term geomagnetic storms for the research presented is made after examination of Disturbed storm-time index, *Dst*, time series, obtained from (http://isgi.unistra.fr/data_download.php). Four recent cases of rapidly developing short-term geomagnetic storms are selected that lasted three days, and are well isolated from similar events in time, as outlined in Table 1. The fifth case of the well-known Halloween 2003 Storm, a massive space weather disruption, is considered a control case in the research.

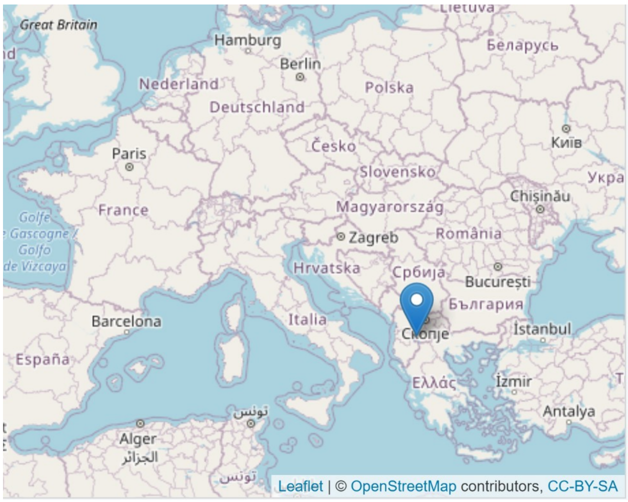

Figure 1. Ohrid, North Macedonia IGS reference station is situated in the mid-latitude region of southern-eastern Europe (7.9°S, 14.8°W), illustration created with our R-based script utilising the *leaflet* R-library, on the background of the Open Street Map layer.

Table 1. Four selected cases of rapidly developing short-term (3-days) geomagnetic storm, and the Halloween 2003 Storm taken as a control case, considered in the research presented

Storm	Start		End	
	Date	DOY	Date	DOY
Storm 1	17MAR15	76	19MAR15	78
Storm 2	27MAY17	147	29MAY17	149
Storm 3	07SEP17	250	09SEP17	252
Storm 4	26SEP17	269	28SEP17	271
Storm 5 (control)	29OCT03	302	31OCT03	304

Time series of TEC within duration of every storm case considered for the Ohrid, North Macedonia reference station are derived from raw dual-frequency GPS observations, and analysed using methodology outlined in Section 2.

4. Research results

Research results are obtained by utilisation of the methodology outlined in Section 2 on the material described in Section 3.
The analysis of Dst sets related to storm cases show clear distinction between rapidly developing short-term geomagnetic storm cases and the massive Halloween 2003 storm, as evident from Figure 2. The latter extends more expanded range of Dst values.

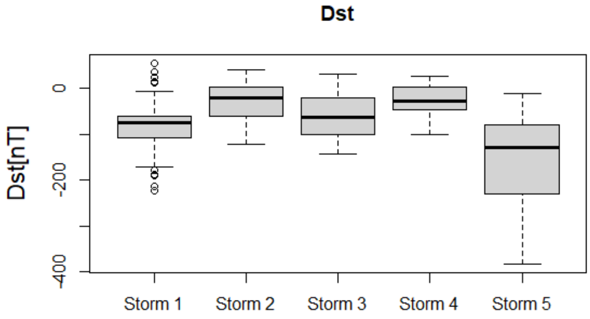

Figure 2. Box-and-whisker plots of Dst values during four rapidly develooing short-term geomagnetic storms and te Halloween 2003 storm.

The similar inference may be drawn from Figure 3, where box-and-whisker plots of derived Ohrid TEC sets are shown for comparison of four cases examined (Halloween 2003 storm TEC value range far exceeds those of Storms 1-4, and is not shown).. Figure 4 shows just four rapidly developing short-term geomagnetic storm TEC box-and-whisker plots, to allow for identification of Storm 1 as the event with the largest TEC values range. Additionally, Storms 3 and 4 extend outliers, as minor disturbances occurred during their geomagnetic storm recovery phases.

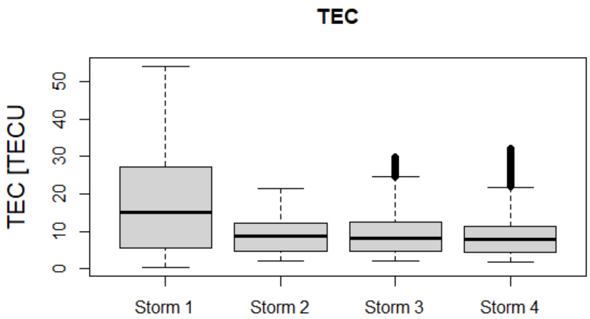

Figure 3. Box-and-shisker plots of Ohrid, NM TEC sets in fours short-term storm cases under observations

Estimates of Shannon entropy for five observed cases are shown in Figure 5. TEC time series observed during rapidly developing short-term geomagnetic storms retain a relatively moderate Shannon entropy levels, not exceeding 0.4, in contrast with the Halloween 2003 storm, as depicted in Figure 5.
Spike index values of TEC time series taken during rapidly developing short-term geomagnetic storm cases, as shown in Figure 6, extend extremely low values, in comparison with the Halloween 2003 storm case (now shown).

5. Discussion

This research assesses statistical properties of TEC time series observed in mid-latitude during with the aim of scenario classification determination in support of tailored TEC prediction model development for mitigation ionospheric effects on GNSS positioning performance (accuracy).

Figure 4. Shannon entropy estimates of Ohrid, NM TEC sets in five cases under observations

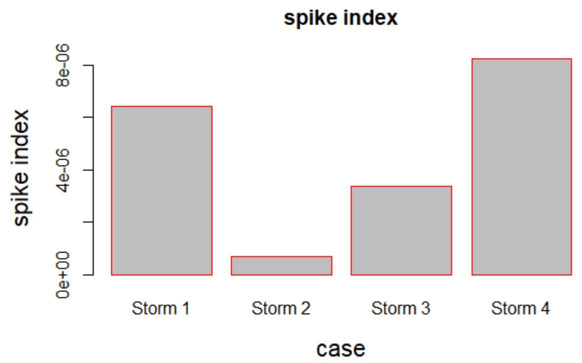

Figure 5. spike index estimates of Ohrid, NM TEC sets in five cases under observations

TEC time series are derived for the Ohrid, North Macedonia IGS reference station for four selected cases of rapidly developing short-term geomagnetic storms with a considerable potential to degrade the GNSS positioning accuracy.

Targeted geomagnetic storm cases are selected by examination of Dst time series.

Exploratory statistical analysis reveals the similarities in box-and-whisker plots of TEC values observed during rapidly developing short-term geomagnetic storm, and the clear distinction with the massive space weather storm taken in this research as a control case. Additionally, the research results stress out the importance of examination of additional disturbances occurring in the deep-through and recovery phases of the original geomagnetic storm, as those disturbances skew the statistical properties and the predictability of the TEC generation process.

TEC times series are examined for their information content in support of TEC prediction model development using Shannon entropy and spike index. Shannon entropy remains at moderate level for TEC time series observed during rapidly developing short-term geomagnetic storms, thus extending reasonable levels of predictability. Similar to the case of exploratory analysis, complexity of geomagnetic conditions, such as those during multiple disturbances, results in a slightly degraded predictability (slightly higher entropy), but within the range that distinguish rapidly developing short-term geomagnetic storm as a separate class of ionospheric-related events, in terms of TEC predictive model development. The observed distinction is supported with the analysis of spike index, which is at negligible levels for all rapidly developing short-term geomagnetic storms under observation, compared with the massive Halloween 2003 storm.

This leads to the conclusion of the correct identification of rapidly developing short-term geomagnetic storm as a separate class of space weather/ionospheric condition scenario, for which a common TEC predictive model may be developed to mitigate GNSS positioning accuracy degradation caused by disturbed ionospheric conditions.

References

[1] M. Filić, "On development of the forecasting model of GNSS positioning performance degradation due to space weather and ionospheric conditions," *Proc 2nd URSI AT-RASC*, 4 pages, Gran Canaria, Spain, May 2018, doi: 10.23919/URSI-AT-RASC.2018.8471628

[2] M. Filić, and R. Filjar, "On correlation between SID monitor and GPS-derived TEC observations during a massive ionospheric storm development," *Proc URSI AP-RASC 2019*, 5 pages, New Delhi, India, doi: 10.23919/URSIAP-RASC.2019.8738664

[3] M. Filić, R. Filjar, "Modelling the Relation between GNSS Positioning Performance Degradation, and Space Weather and Ionospheric Conditions using RReliefF Features Selection," *Proc ION GNSS+ 2018*, 1999-2006, Miami, FL, doi: https://doi.org/10.33012/2018.16016

[4] R. Filjar, M. C. Damas, and T. B. Iliev, "Resilient Satellite Navigation Empowers Modern Science, Economy, and Society," *IOP Conf. Ser: Mater Sci Eng*, **1032**, 012001, 2021, 10 pages, doi:10.1088/1757-899X/1032/1/012001

[5] R. J. Hyndman, and G. Athanasopoulos, Forecasting: Principles and Practice (3rd ed), 2021. Available at: https://otexts.com/fpp3/

[6] J. Sanz Subirana, J. M. Juan Zornoza, and M. Hernández-Pajares, GNSS Data processing, Volume 1: Fundamentals and Algorithms. Nordwijk, The Netherlands: ESA. ISBN 978-92-9221-886-7